Hydrophobic chains near hydrophobic surfaces—simulations in three dimensions

2005 J. Phys.: Condens. Matter 17 S1183

(http://iopscience.iop.org/0953-8984/17/14/007)

INSTITUTE OF PHYSICS PUBLISHING JOURNAL OF PHYSICS: CONDENSED MATTER

J. Phys.: Condens. Matter **17** (2005) S1183–S1194 doi:10.1088/0953-8984/17/14/007

Hydrophobic chains near hydrophobic surfaces—simulations in three dimensions

Yasemin Şengün[1] **and Ayşe Erzan**[1,2]

[1] Department of Physics, Faculty of Sciences and Letters, Istanbul Technical University, Maslak 34 469, Istanbul, Turkey
[2] Gürsey Institute, POB 6, Çengelköy, 34 680 Istanbul, Turkey

Received 7 September 2004, in final form 7 December 2004
Published 24 March 2005
Online at stacks.iop.org/JPhysCM/17/S1183

Abstract

The behaviour of a hydrophobic chain near a hydrophobic wall is studied in three dimensions by numerically simulating a modified version of the decorated lattice model of Widom and co-workers. The effective hydrophobic interaction is temperature dependent. The chain stretches and adheres to the hydrophobic wall in a pancake like conformation at intermediate temperatures, whereas it collapses upon itself at slightly higher temperatures. At lower or higher dimensions it is in a random coil state.

1. Introduction

The hydrophobic effect is of central importance in driving many biological processes, in particular the folding of protein chains [1–5]. Yet it is still an active topic of research, with contending theories attempting to capture many different, and seemingly conflicting phenomena associated with it [6–12]. It is a challenge to identify the microscopic mechanisms at work, and to apply them to understanding the behaviour of hydrophobic macromolecules within an aqueous medium and confined near hydrophobic surfaces, such as lipid membranes, at different temperatures.

The decorated lattice model of hydrophobic interactions introduced by Widom and co-workers [11] aims to capture the entropy-mediated nature of the 'hydrophobic interaction.' This means that the non-polar (hydrophobic) molecule may enter an attractive interaction with the water molecules, through dipole–induced dipole (van der Waals) interactions, even though one would expect that the energy cost of inserting a hydrophobic solute molecule into water would be positive, due to the breaking of hydrogen bonds between water molecules. If the low energy state of the water–hydrophobe system corresponds to highly ordered configurations of the water molecules, which allow this insertion without the breaking of too many hydrogen bonds, then the entropy cost will be too great, and the free energy minimum will be found in a phase space region where the hydrophobes are segregated from the water, at least in some temperature interval.

In the original model [11], hydrophobic molecules are not allowed to mix with water molecules in the orientationally 'disordered' state of the water. In two parallel papers [13, 14] we developed a slightly modified version of the Widom model, where all energies considered are finite, and applied it to the statistics of hydrophobic chains in two dimensions. Analytical calculations [13] and simulations [14] yielded a consistent picture, with the hydrophobic chain adhering closely to the hydrophobic wall over a certain temperature interval, collapsing upon itself at slightly higher temperatures, and existing in a random coil state at temperatures that are either too hot or too cold.

In the present paper, we will report simulations of the same system generalized to three dimensions. Since the 'hydrophobic interaction' itself is an entropy mediated one, with many competing effects due to the orientational entropy of the water molecules and the configurational entropy of the hydrophobic chain, it is not *a priori* clear how the emerging picture will be affected by a change in the dimensionality of the lattice on which the calculations are performed. Here, as in [14], we performed genetic algorithm (GA) computations [15] to probe the low energy states, and Metropolis Monte Carlo (MC) [16, 17] for the equilibrium values of quantities such as the centre of mass distance from the wall, the radius of gyration, the internal energy and the free energy. The qualitative picture remains very similar to what we find in two dimensions.

The paper is organized as follows. In section 2, we extend our model for a hydrophobic chain interacting with a hydrophobic wall [13, 14] to three dimensions. In section 3, we outline the methods used and report our results. Section 4 summarizes our conclusions.

2. Hydrophobic interactions within the decorated lattice model

In the decorated lattice model [11, 13] for hydrophobic interactions, water molecules occupy the lattice sites, and the hydrophobic solute particles, represented by lattice gas variables $\sigma_{ij} = 0, 1$, decorate the bonds. Each water molecule can be in one of many orientational states, and is represented by Potts spins, s_i, which can take on q different values. The Hamiltonian is

$$H = \sum_{\langle ij \rangle} \{\delta_{s_i,s_j}\delta_{1,s_i}[\sigma_{ij}(w-u)+u] + v\sigma_{ij}[1-\delta_{s_i,s_j}\delta_{1,s_i}]\}, \tag{1}$$

where the interaction energies have been chosen as $w = -1.5$, $u = -1$, $v = 1$ and $q = 10$ unless otherwise specified. This Hamiltonian corresponds to a situation where it is energetically favourable, due to dipole–induced dipole interactions, for the hydrophobic molecules to be interspersed among the water molecules, for a locally ordered state of the water molecules where this insertion can be accomplished without breaking too many hydrogen bonds. This ordered state is represented by requiring the neighbouring Potts spins to be set to $s_i = 1$, and if there is a hydrophobe present to decorate the bond, one gets a contribution of w. If there is no hydrophobe present, then this locally ordered state still has lower energy (u) than the situation where some of the hydrogen bonds are broken, or the local order has given way to complete disorder. This latter case has been chosen as the zero point of the energy. Finally, introducing a hydrophobe into the completely disordered array of water molecules costs an energy of solvation equal to v. The rationale behind the energy scale is that we assume the 'ordered, no hydrophobe' and 'disordered, with hydrophobe' states to differ from the 'disordered, without hydrophobe' state by about the same number of hydrogen bonds (each $\sim$17 eV), thus suggesting $|u| = v$, whereas the van der Waals interaction (further lowering the energy in the 'ordered, with hydrophobe' situation) has perhaps been somewhat overestimated with our choice of $w - u = -0.5$. Thus the natural unit of energy here is of the order of a hydrogen bond per water molecule.

For sufficiently high temperatures T, the free energy $F = U - TS$ is more efficiently lowered by raising the entropy S than by lowering the internal energy U. Raising the orientational disorder of the water molecules, modelled by the Potts spins, is the most efficient way of raising the total entropy of the system. This makes it unlikely for the hydrophobes to intermix with the water in the equilibrium state. For yet higher temperatures, where the internal energy itself is large, the totally intermixed situation is once more the equilibrium state. Finally, note that larger values of q will lead to a more pronounced entropic effect, and therefore stronger 'hydrophobic interactions' [13, 14].

It is easy to see that the maximal number of water molecules that can be constrained by N hydrophobes in the low energy state is $2N$, independently of the lattice dimensionality, when the hydrophobes are dilute and randomly distributed. When they form a compact set on the shifted lattice which they occupy, this number is of the order of N (since each hydrophobe decorates a unit vector of the lattice on which the water molecules live), neglecting surface effects.

To be able to cut down on computation time when simulating a chain of length N, while respecting chain connectivity, we made use of an analytical mean-field type of approximation [13] to the effective hydrophobic interactions between nearest neighbour (nn) or next nearest neighbour (nnn) hydrophobic residues on the chain. Consider a water molecule at some typical lattice site i. Let $t_i \equiv \delta_{s_i,1}$. The $2d$ bonds emanating from this site are decorated by the lattice gas variables σ_j corresponding to the hydrophobes and the t_j terminating the $2d$ bonds are set to their thermal averages. The mean field Hamiltonian for this system may be written (dropping the i dependence) as

$$H_{\mathrm{MF}} = \sum_{j=1,\ldots 2d} \{t\langle t\rangle[\sigma_j(w-u-v)+u]+\sigma_j v\} - \beta^{-1}\mu(1-t)\ln(q-1), \tag{2}$$

where μ will eventually be set to unity. Note that $\langle t\rangle$ is related to the orientational order parameter for the water molecules, which could have been defined as $(q\langle t\rangle - 1)/(q-1)$, to range between 0 and unity. The value of $\langle t\rangle$ for each β is calculated self-consistently from

$$1 - \langle t\rangle = [\ln(q-1)]^{-1}\frac{\partial}{\partial\mu}\ln Z|_{\mu=1}, \tag{3}$$

where

$$Z = \sum_{\{\sigma_i\},t} \mathrm{e}^{-\beta H_{\mathrm{MF}}[t,\{\sigma_i\}]}. \tag{4}$$

To obtain the effective pair interactions $M(\beta)$, we sum over the t in this expression, and equate the result to a sum over Boltzmann factors involving an effective Hamiltonian, expanded in terms of products of the lattice gas variables σ_j [13]. Neglecting the higher order interactions, which in three dimensions will go beyond the plaquette interaction, all the way to a term involving all the six hydrophobic lattice gas variables surrounding a central water molecule, we find,

$$\mathrm{e}^{\beta M(\beta)} = [(q-1)\mathrm{e}^{-2\beta v} + \mathrm{e}^{-\beta\{\langle t\rangle[2(w-v)+(2d-2)u]+2v\}}]\frac{(q-1)+\mathrm{e}^{-\beta 2d\langle t\rangle u}}{[(q-1)\mathrm{e}^{-\beta v}+\mathrm{e}^{-\beta\{\langle t\rangle[(w-v)+(2d-1)u]+v\}}]^2}.$$

To obtain the potential acting on each hydrophobe due to the presence of the hydrophobic wall, we make use of dimensional reduction. The two-dimensional wall of infinite extension (compared to the size of the molecules, or chains) suggests solving the decorated lattice model exactly in one dimension, as a function of the normal distance to the wall [13]. This effective potential is calculated as the free energy cost $F(\beta, r)$ of introducing a hydrophobe (at the position r) into a semi-infinite chain, with one end fixed to be hydrophobic. The hydrophobic 'force' $f(\beta, r) = -\partial F(\beta, r)/\partial r$ per hydrophobic residue as a function of the distance from

the hydrophobic wall extends up to six lattice spacings for $\beta = 2$, and is appreciable at smaller distances within the approximate range $1 < \beta < 3$ (see figure 3 of [14].) The attraction is stronger for larger q. The size of the temperature interval within which the interaction is appreciable, and of comparatively longer range, also increases with q. In this paper we have confined ourselves to $q = 10$.

In all the simulations to be reported in the next section, the energy differences between different configurations and the Boltzmann weights for the thermal averages were computed by making use of the effective interactions $M(\beta)$ and $F(\beta, r)$, such that the effective Hamiltonian on the lattice was

$$H_{\text{eff}} = -\sum_{(ij)} M(\beta) + \sum_{i=1,\ldots,N} F(\beta, r_i), \tag{5}$$

where (ij) denotes all nn and nnn pairs on the chain (excluding the chemically connected ones) and r_i denotes the distance of the ith residue from the hydrophobic wall.

3. Simulations

We have performed Monte Carlo (MC) and genetic algorithm (GA) simulations to investigate the thermal equilibrium and the low energy states, respectively, of the hydrophobic chains in the vicinity of a hydrophobic wall. Here we would like to outline our simulation methods, which have been explained in great detail in [14], and to report the results of simulations in three dimension.

The Metropolis Monte Carlo method is guaranteed, in principle, to converge to the equilibrium distribution [16, 17]. However, in many problems of interest, which involve a large degree of frustration and consequently a very rugged energy landscape, very long-lived metastable states and a large degeneracy of the ground state require special techniques to achieve proper equilibration within reasonable computation times. We found that the present problem exhibits a great degree of ground state degeneracy or near-degeneracy, due to purely geometrical effects. Therefore it is worthwhile to try to investigate the low-lying energy states, separately.

There are some well established schemes [17] for Monte Carlo simulations of flexible chains, in particular the so-called 'configurational bias Monte Carlo' [18]. In this approach, the molecular chain configurations are grown in such a way that each successive residue is added according to a Gibbsian probability distribution defined over the available sites where the growth can occur, and new conformations are generated by cutting back a chain at some random point and regrowing it. In our case, this would have entailed regrowing the whole ensemble of chains from scratch for each temperature, since the Boltzmann factors here depend not only explicitly, but also implicitly on the temperature, through the effective, temperature dependent 'Hamiltonian,' equation (5), for both intra-chain interactions, and the external potential [19]. So what we have done is to generate an ensemble of random self-avoiding chain configurations, and subjected the chains to *moves* such as 'crossovers' and 'mutations' as defined below. Different protocols for the selection of the chains, and acceptance or rejection of a move, depended on whether we were optimizing with respect to the energy (GA) or trying to achieve thermal equilibrium (MC).

3.1. Methods

The genetic algorithm [15], which is widely used in very high dimensional optimization problems, is inspired by the genetic processes underlying natural selection. The moves are

based upon the mutation of the linear code corresponding to a given individual in the population, and the mixing, by means of a crossover operation, of the linear codes corresponding to two different individuals. In this paper, *crossover* means that the sequence of numbers specifying two selected configurations are interchanged onwards from a randomly chosen point. *Mutation* of a chain means that the number specifying the relative orientation of a randomly chosen director is changed randomly. Since the problem is invariant under translations parallel to the wall, *translations* are performed in the direction perpendicular to the wall. A *rotation* is like a mutation operation, but the director whose code is to be modified is the first in the sequence. We have checked that all these operations conserve the connectivity of the chain.

In the course of MC simulations, we have used mutation, as well as translation and rotation, to generate different chain configurations.

Both the MC and the GA procedures as we have implemented them [14] start out from an initial population of random self-avoiding chain configurations. An ensemble of single random chains of fixed length N, confined to a volume bounded by a pair of parallel walls, and having periodic boundary conditions in the other directions, was grown step by step from random initial positions, and with random initial orientations, requiring only that they do not self-intersect, or collide with the walls.

A genetic algorithm step for evolving the population so that it inhabits the lowest energy states of the system is effected in the following way. We select two configurations from the current chain population, with probabilities proportional to a fitness function, which here we have chosen to be equal to their Boltzmann weights, $\exp(-\beta H_{\text{eff}})$. We perform crossover at a randomly chosen point in the two sequences of numbers characterizing the two chain configurations; mutate the resulting two configurations by randomly modifying a number at a randomly chosen point in each of the two sequences, as well as translating and rotating each chain randomly; and finally we remove two randomly chosen individuals from the population. This constitutes one step of the GA.

A Monte Carlo step consists of *randomly* selecting a chain configuration from the current chain population, randomly picking one of the operations of translation, rotation or mutation (with the same meanings as for the GA), checking that the resulting configuration does not intersect itself or a wall, calculating the effective energy difference, ΔE, then accepting or rejecting the new configuration according to the Metropolis criterion, and repeating this until the whole population is exhausted.

In two dimensions, we tried also prefacing the MC relaxation with a GA calculation, so that for each temperature, the relaxation started from a set of relatively low energy configurations. After the same number of steps as that used to relax from a random set, we found that the ensemble still retained to some extent certain features of the optimized set [14]. This could be due to the fact that the ensemble has not yet completely equilibrated; and therefore we have decided to avoid this here. We simply report the results of the GA or the MC procedures, with the random population of self-avoiding chains on the lattice as the starting population.

3.2. Simulation parameters

The simulations were performed with a hydrophobic chain with $N = 20$ hydrophobic residues placed on nearest neighbour positions on a $2N \times 2N \times 2N$ cubic lattice of unit lattice spacing. One boundary of the lattice is taken to be a hydrophobic wall and the opposite boundary is just a simple infinite barrier. The other four sides of the cubic lattice satisfy periodic boundary conditions.

A chain configuration (or walk) is labelled by a string of numbers starting with the three coordinates of the chain, a number to indicate the Cartesian direction of the first step, and then a sequence of numbers each indicating the director of the $(n+1)$th step relative to the nth. They are chosen such that the $(n+1)$th director can take on the values $a_{n+1} = 1, 2, \ldots, 5$, with 1 indicating the same direction as that of the step from the $(n-1)$th site to the nth (backfolding of the walk is prohibited). If this step is in the positive or negative $\hat{x}$ direction, then the rest of the possible directions are assigned a_{n+1} values according to the ordered pairs $(2, \hat{y})$, $(3, -\hat{y})$, $(4, \hat{z})$, $(5, -\hat{z})$. For other values of the director a_n, e.g., $-\hat{x}$, $\hat{y}$ etc, the pairing of the Cartesian unit vectors is cyclically permuted. Only self-avoiding chain configurations on the lattice, which also avoid intersection with any of the walls, are accepted. This representation is convenient for performing the crossover and mutation operations under the genetic algorithm or the Monte Carlo simulations.

Unless stated otherwise, all results are reported for an initial set of 10^3 random configurations (whose positions and orientations have also been randomized) relaxed for 4×10^4 steps, and averaged over the last 5×10^3 steps. For each temperature, the same set of 10^3 random configurations has been taken as the starting distribution. The error bars correspond to one standard deviation computed over the last 5×10^3 steps of the iteration. The error bars for the GA calculations are frequently smaller than the size of the symbols and therefore invisible in the figures. For the GA computations, we report the Boltzmann weighted averages over the set of lowest energy configurations to which the algorithm has converged. The results of the MC calculations correspond to the thermal averages performed over the equilibrated set of chains.

3.3. Results

We have demonstrated for two dimensions [14] that, since the distribution evolving under the GA is more localized in energy, it is very close to being a microcanonical ensemble. Thus, for the GA, the thermal average for observables such as the centre of mass displacement from the wall, the radius of gyration, etc, almost coincide with the simple average taken over the ensemble. This we also expect to be true for $d = 3$.

In figure 2 we see that the effective interaction with the wall, $F(\beta, r)$, drives the chain to within a few lattice spacings of the wall. The centre of mass displacement $\langle r_{\rm cm} \rangle$ from the wall is very small, i.e., the chain adheres to the wall over a larger temperature interval (approximately $\beta \in (0.7, 3.0)$) for the low energy configurations (GA), while in thermal equilibrium (MC) this interval is narrower (approximately $\beta \in (1.0, 2.5)$). Outside this interval, the centre of mass of the chain is precisely at mid-channel. Note that the low energy configurations obtained by the GA for the centre of mass displacement, $\langle r_{\rm cm} \rangle$, in the region $\beta \in (0.3, 0.7)$ are plagued by large fluctuations; this is the region where the chain has collapsed upon itself as can be seen from the dip in the radius of gyration, $\langle R_{\rm g} \rangle$, in figure 3. Comparing with the results in two dimensions [14], we find that qualitatively the picture is very similar. However, the lower limit of the β interval over which the chain adheres to the wall is slightly smaller in three dimensions.

From figure 3, we see that the radius of gyration $R_{\rm g} = [N^{-1} \sum_{i=1,\ldots,N} \rho_i^2]^{1/2}$, where ρ_i is the distance of the ith residue from the centre of mass of the chain, is somewhat smaller than for a self-avoiding walk (SAW) in three dimensions, of the same length, namely $N^{3/5}/2$, and slightly larger than for a random walk, $N^{1/2}/2$. For $\beta \simeq 0.5$ where the nearest neighbour effective interactions are strongest (cf figure 1), we see that the radius of gyration shrinks markedly and systematically. By contrast, in the interval where the chain is attracted to the wall, the sample to sample variations in $\langle R_{\rm g} \rangle$ are quite large, leading to large error bars in both the GA and MC simulations.

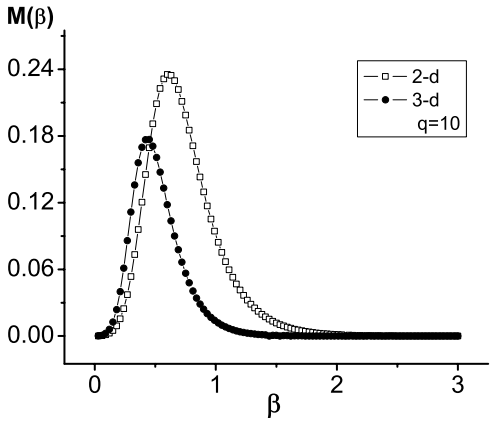

Figure 1. Effective two-body interaction calculated self-consistently in the mean field approximation in two and three dimensions, as a function of the inverse temperature, β. The peak is shifted to slightly higher temperatures (lower β) and the width of the maximum is diminished as one goes from two to three dimensions.

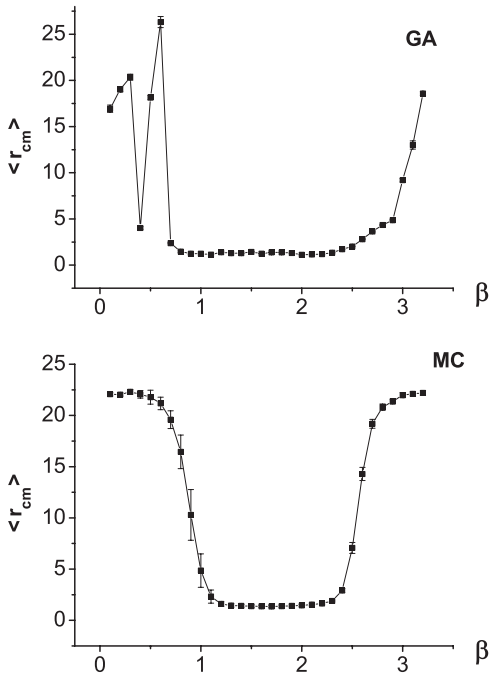

Figure 2. The centre of mass displacement of a hydrophobic chain from a hydrophobic wall, averaged over 5×10^3 steps after 3.5×10^4 relaxation steps, as a function of the (dimensionless) inverse temperature, β, obtained via the genetic algorithm and Metropolis Monte Carlo calculations (see the text). The parameter values in all the figures are $w = -1.5$, $u = -1$, $v = 1$.

It should be remarked that the two contributions to the Hamiltonian in equation (5), namely the self-interaction of the chain and the interaction with the wall, come from different kinds of approximations to the true problem. Therefore the relative size and the positioning of the temperature intervals over which these two kinds of interactions are dominant should be taken

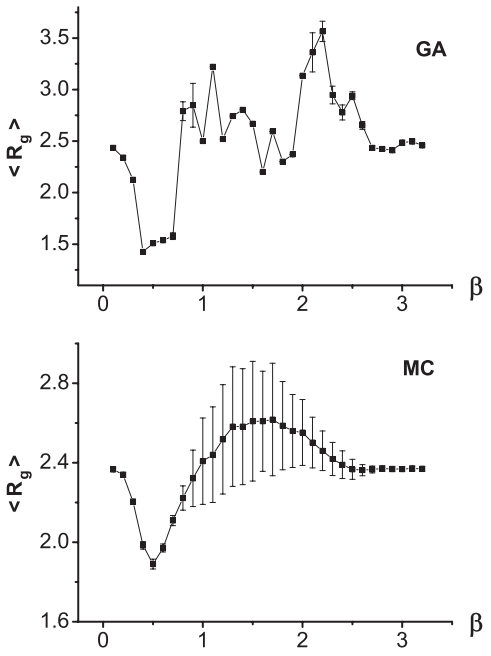

Figure 3. The radius of gyration obtained from genetic algorithm and Monte Carlo simulations.

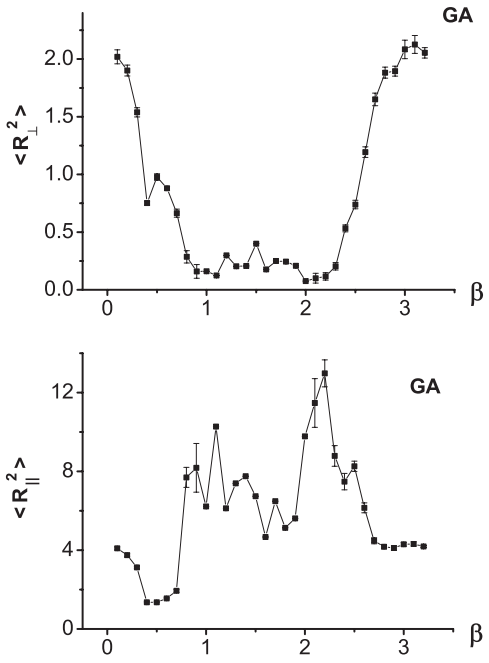

Figure 4. The radius of gyration in the direction perpendicular and parallel to the wall, for low energy configurations, obtained via the genetic algorithm.

with some caution. Nevertheless, it is gratifying that the relative width and especially the order of these intervals does not change when one goes from two dimensions [14] to three.

It is interesting to compare the results for $\langle R_{\rm g}\rangle$ with those shown in figures 4, 5 for the radii of gyration in the directions parallel and perpendicular to the wall, namely $R_\parallel = [N^{-1}\sum_{i=1,\ldots,N}\rho_{\parallel i}^2]^{1/2}$, and $R_\perp$ defined in an analogous way. This shows that in the region where the chain is attracted to the wall, it gets extended in the parallel directions while it shrinks in the perpendicular direction, confining itself to a pancake-like region near the wall. Another quantity of interest is the length of the projection of the chain on the wall, $\langle L_\parallel = (L_x^2 + L_y^2)^{1/2}\rangle$. A comparison of figure 6 with figure 2 and figures 4, 5 reveals that in the temperature interval where the chain adheres closely to the wall, it will be relatively stretched out, as can also be seen from $\langle R_\parallel\rangle$. Note that, contrary to the case of the centre of mass displacement of the collapsed chain, for the radii of gyration, the fluctuations are prominent in the region of close approach to the wall.

In figure 7 the internal energy of the chain and free energy are shown. We see three temperature intervals where the behaviour seems to differ qualitatively. The sharp minimum in energy in the region where the first term in the Hamiltonian (equation (5)) is dominant, is very pronounced, whereas in the region where the attraction to the wall (the second term in the Hamiltonian) is dominant, there are big sample to sample fluctuations due to the fluctuation in $\langle L\rangle$ and $\langle R_{\rm g}\rangle$. We can also compute an effective 'free energy' for the ensemble of chains in the vicinity of the wall,

$$F_{\rm eff} = -\beta^{-1}\ln Z_{\rm chain}, \tag{6}$$

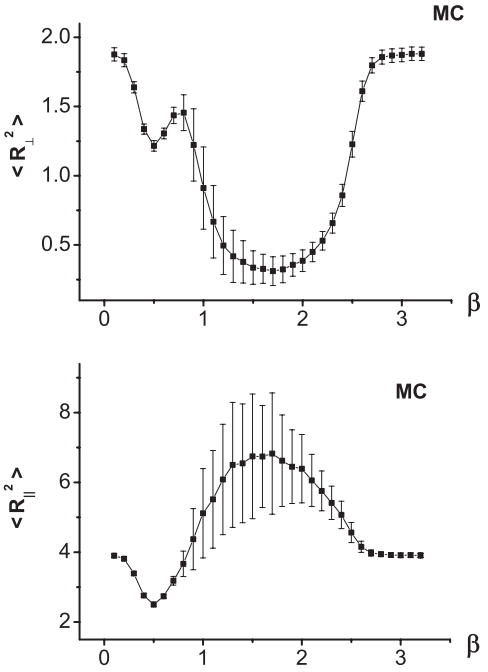

Figure 5. The thermal average of the radius of gyration in the direction perpendicular and parallel to the wall, from Metropolis Monte Carlo.

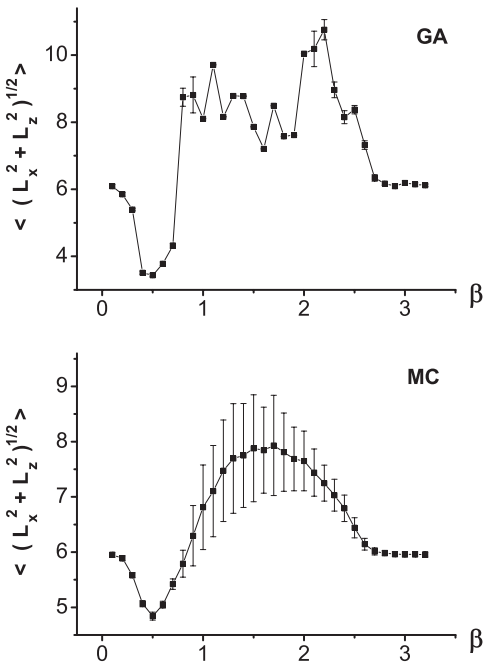

Figure 6. The thermal average of the projected length $L_\parallel = (L_x^2 + L_y^2)^{1/2}$ of the chain on the wall. The first and second panel correspond to the genetic algorithm and Monte Carlo simulations respectively.

where

$$Z_{\text{chain}} = \sum_{\text{config.}} \exp(-\beta H_{\text{eff}}[\text{config.}]). \tag{7}$$

Because of the compensating terms, namely the internal energy and the entropic term, in the expression for the free energy, this last quantity is almost free of sample to sample fluctuations, as can be seen from figure 7. Although it would seem that this free energy is plagued by instabilities, i.e., regions where it is not convex with respect to the temperature, it should be noted that this effective free energy is not the total free energy of the system we started out with. In particular it does not include the fluctuations in the number of hydrophobic particles. (We have checked, by exactly enumerating the configurations on a 2×2 lattice, that the residual negativity in $\partial^2 F/\partial T^2$ is not coming from insufficient equilibration of the chains.)

In order to check the consistency of our results, we have also done simulations where the initial random set was evolved to equilibrium at high temperature, and then the temperature gradually lowered for each successive data point. The system is then slowly heated until the initial temperature is reached. We report the MC results thermally averaged over 1000 configurations, and averaged over the last 5×10^3 steps of a trajectory of 2×10^4 steps, in figures 8, 9. The error bars have been omitted from these figures for greater clarity. For quantities where the fluctuations are relatively large, such as the projected length, or the radius of gyration, there are slight differences in the thermal averages between the cooling and the heating curves. On the other hand, the centre of mass distance from the wall, internal energy or free energy show almost no hysteretic effects at all.

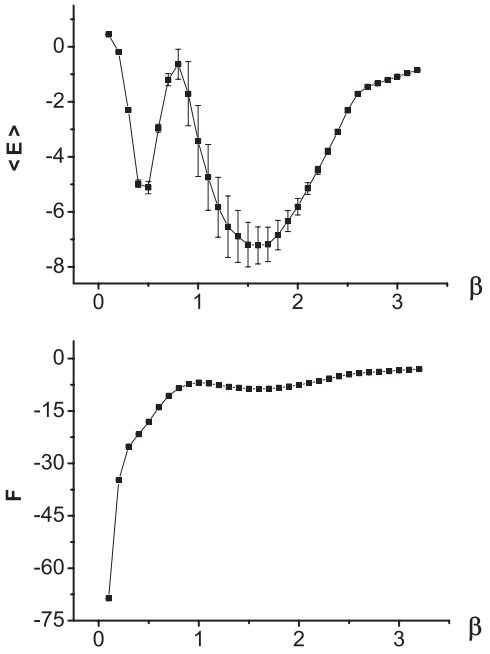

Figure 7. The internal energy and the free energy as a function of the inverse temperature, from Monte Carlo calculations.

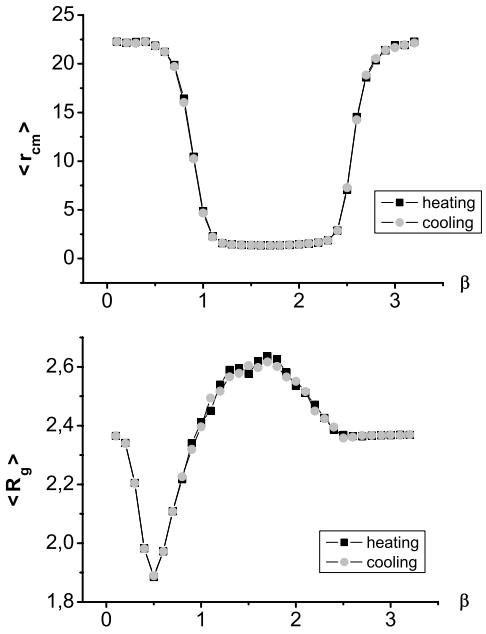

Figure 8. The cooling and heating curves (Monte Carlo simulations) for the centre of mass distance from the wall, and the radius of gyration. The curves are practically indistinguishable from each other for $\langle r_{\rm cm}\rangle$, while for the radius of gyration, which exhibits greater fluctuations, there is a very small hysteresis.

4. Conclusions

We set out to investigate the behaviour of a system consisting of a hydrophobic chain in a three-dimensional aqueous environment, bound on one side by a hydrophobic wall. An extension of the decorated lattice model of Widom *et al* [11, 13, 14] was employed, and numerical simulations were carried out on a three-dimensional lattice. We found that within a certain temperature interval the chain binds on to the hydrophobic surface in a relatively stretched out and flattened conformation, and at a slightly higher temperature interval it unbinds from the surface and collapses onto itself, with a radically lower radius of gyration. More accurate estimations of the short range hydrophobic intra-chain and chain–wall interactions are called for, to make more reliable statements; nevertheless, our results should be of interest for understanding the interaction between proteins and lipid surfaces.

Apropos of the problem of protein folding, the picture we obtain is suggestive of a chaperoning function provided by the hydrophobic surface [20]. In fact, there exist studies which reveal that the chaperoning action of the protein 'chaperonin' can be simply modelled by the confinement of the protein inside a cylindrical cavity with hydrophobic walls [21]. Apparently, confinement inside a cage can already accelerate folding rates for (shorter) proteins with relatively small amount of frustration [22], while for longer proteins, the hydrophobicity of the wall is crucial [21].

We have already remarked that since different approximations have been made to model the chain–wall and intra-chain interactions, the relative positions of the temperature intervals

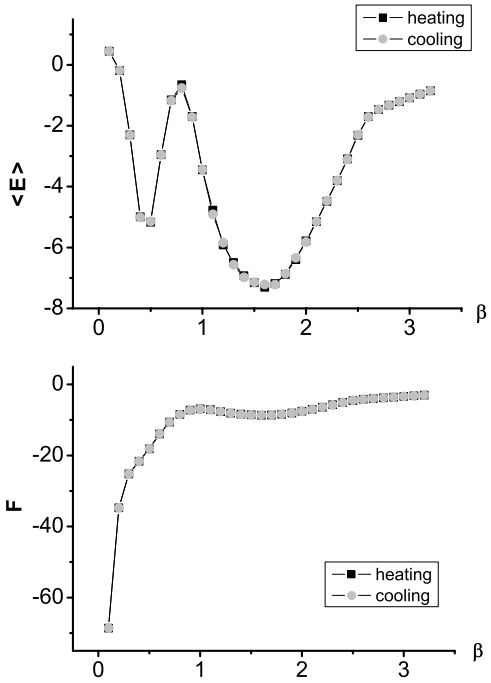

Figure 9. The cooling and heating curves obtained from MC simulations for the internal energy and the free energy follow exactly the same trajectory.

we find here should be taken with some caution. Nevertheless, in the static picture presented here, the presence of adjacent temperature intervals, where hydrophobic residues bind onto a hydrophobic surface, and where the chain is collapsed onto itself, suggest that a cycling of the temperature could very well lead to the effective sampling of alternate pathways. In particular, coming from the side of low temperatures, first binding onto the hydrophobic surface in a stretched out formation could facilitate the correct folding as the temperature is slightly increased. Considering chains with both hydrophobic and polar residues (rather than the purely hydrophobic chains we have considered here) makes this more likely. In this case, one could argue heuristically that the flattened conformation against the wall would have the hydrophobes predominantly closer to the wall. As the temperature is slightly raised, and the chain detaches from the wall, one has an easy pathway for the already relatively segregated hydrophobes to fold up into the core of the collapsed conformation.

Acknowledgments

The numerical computations were performed on the Gilgamesh Cluster Project at the Feza Gürsey Institute. AE would like to thank the organizers, M R H Khajehpour and Ramin Golestanian of the Conference on Complex Fluids, at the Institute of Advanced Studies in the Basic Sciences, Zanjan, as well as Roland Netz, Rama Cont and Janos Kertesz for interesting and useful remarks. She would also like to gratefully acknowledge partial support by the Turkish Academy of Sciences.

References

[1] Ben-Naim A 1980 *Hydrophobic Interactions* (New York: Plenum)
[2] Ben-Naim A 1989 *J. Chem. Phys.* **90** 7412

[3] Frauenfelder H, Sligar S G and Wolynes P G 1991 *Science* **254** 1598
[4] Sali A and Shakhnovich E 1994 *J. Mol. Biol.* **235** 1614–36
[5] Dill K A *et al* 1995 *Protein Sci.* **4** 561–602
[6] ten Wolde P R 2002 *J. Phys.: Condens. Matter* **14** 9445
[7] ten Wolde P R and Chandler D 2002 *Proc. Natl Acad. Sci.* **99** 6593
[8] Huang D M and Chandler D 2000 *Proc. Natl Acad. Sci.* **97** 8324
[9] Mamatkulov S I, Khabibullaev P K and Netz R R 2004 *Langmuir* **20** 4756
[10] Netz R R 2004 *J. Phys.: Condens. Matter* **16** S2353
[11] Barkema G T and Widom B 2000 *J. Chem. Phys.* **113** 2349
Schtz G M, Ispolatov I, Barkema G T and Widom B 2001 *Physica* A **291** 24
Bedeaux D, Koper G J M, Ispolatov I and Widom B 2001 *Physica* A **291** 39
Widom B, Bhimalapuram P and Koga K 2003 *Phys. Chem. Chem. Phys.* **5** 3085
[12] Israelachvili J and Wennerstrom H 1996 *Nature* **379** 219
[13] Önder P and Erzan A 2002 *Eur. Phys. J.* E **9** 467
[14] Şengün Y and Erzan A 2004 *Proceedings, Macromolecules 2004 (Paris, July 2004)* (*Eur. Phys. J.* E submitted to special issue)
[15] Holland J H 2001 *Adaptation in Natural and Artificial Systems* (Cambridge, MA: MIT Press)
[16] Binder K and Heermann D W 1997 *Monte Carlo Simulations in Statistical Physics* (Berlin: Springer)
[17] Frenkel D and Smit B 1996 *Understanding Molecular Simulation* (San Diego, CA: Academic)
[18] Siepmann J I and Frenkel D 1992 *Mol. Phys.* **75** 59
[19] Inda M A and Frenkel D 2004 *Macromol. Theory Simul.* **13** 36
[20] Erzan A and Tüzel E 2003 *Braz. J. Phys.* **33** 573
Tüzel E and Erzan A 2004 *Ari* **54** 19 (*Preprint* cond-mat/0107315)
[21] Jewett A I, Baumkertner A and Shea J-E 2004 *Proc. Natl Acad. Sci. USA* **101** 13192
[22] Takagi F, Koga N and Takada S 2003 *Proc. Natl Acad. Sci. USA* **100** 11367